Research Square

Preprints are preliminary reports that have not undergone peer review.
They should not be considered conclusive, used to inform clinical practice,
or referenced by the media as validated information.

Data-Independent Acquisition-Based Quantitative Proteomic Analysis of m.3243A>G MELAS Reveals Novel Potential Pathogenesis and Therapeutic Targets

Xueli Chang
First Hospital of Shanxi Medical University
Wei Zhang
First Hospital of Shanxi Medical University
Chuanqiang Pu
Chinese PLA General Hospital
Qiang Shi
Chinese PLA General Hospital
Juan Wang
First Hospital of Shanxi Medical University
Jing Zhang
First Hospital of Shanxi Medical University
Li Yan
First Hospital of Shanxi Medical University
Wenqu Yang
Shanxi Datong University
Hui Zhang
First Hospital of Shanxi Medical University
Junhong Guo (✉ neuroguo@163.com)
First Hospital of Shanxi Medical University

Research

Keywords: mitochondrial myopathy, encephalopathy, lactic acidosis and stroke like episodes (MELAS), skeletal muscle, proteomics, DIA

Posted Date: July 2nd, 2020

DOI: https://doi.org/10.21203/rs.3.rs-38357/v1

License: This work is licensed under a Creative Commons Attribution 4.0 International License. Read Full License

Abstract

Background

The pathogenesis of mitochondrial myopathy, encephalopathy, lactic acidosis and stroke like episodes (MELAS) syndrome is not completely understood. The m.3243A > G mutation responsible for 80% MELAS patients affects proteins with undetermined functions. Therefore, we performed quantitative proteomic analysis on skeletal muscle specimens from MELAS patients.

Methods

We recruited 10 patients with definitive MELAS and 10 controls matched by age and gender of MELAS patients for comparison. We performed nanospray liquid chromatography-mass spectrometry (LC-MS) based proteomic analysis in the data-independent acquisition (DIA) modes, followed by the statistical analysis to reveal the differentially expressed proteins.

Results

We identified 128 differential proteins between MELAS and controls, including 68 for down-regulation and 60 for up-regulation. We studied the differential proteins involved in oxidative stress and indicated a highly significant up-regulation of heat shock protein beta-1 (HSPB1), alpha-crystallin B chain (CRYAB) and heme oxygenase 1 (HMOX1) but a decrease of glucose-6-phosphate dehydrogenase (G6PD) and selenoprotein P (SEPP1). KEGG pathway analysis and gene ontology (GO) evaluation revealed that the phagosome, proliferator-activated receptors (PPAR) signaling pathway and ribosome showed significant enrichment.

Conclusions

The results revealed that the imbalance between oxidative stress and antioxidant defense, activation of autophagosomes and abnormal metabolism of mitochondrial ribosome proteins played an important role in m.3243A > G MELAS. The combination of proteomic profiling and bioinformatics analysis could contribute novel molecular networks to the pathogenesis of MELAS in a comprehensive manner.

1. Introduction

The mitochondrial diseases are one of the most common congenital metabolic defects, with a minimum prevalence of 1:5000[1, 2]. Mitochondrial myopathy, encephalopathy, lactic acidosis and stroke like episodes (MELAS) is one of the relatively common mitochondrial diseases affecting the central nervous system. MELAS can affect multiple systems, with a wide range of clinical manifestations including stroke, recurrent headaches, epilepsy, hearing impairment, myopathy, dementia, ataxia and diabetes[3]. Almost 80% of MELAS patients are caused by the m.3243A > G mutation in the MT-TL1 gene[4, 5]. The mutation disturbs mitochondrial protein synthesis and ultimately affect the assembly of Complexes I, III and IV on oxidative respiration chains[6]. The molecular mechanism underlying the pathogenesis of MELAS is not fully understood. Finding out more

effective diagnostic methods, and fully understanding the pathogenesis at molecular level, can prevent and reduce the complications of MELAS in a more effective manner.

Mitochondrial proteome is co-encoded by mtDNA and nuclear genome. The mtDNA only encodes 13 OXPHOS proteins; the nuclear genome encodes the remaining roughly 1500 protein and these proteins are transferred to the mitochondria through complex import systems[7]. The mutations of mitochondrial diseases affect proteins with undetermined functions. These proteins might shed light on the pathogenesis of mitochondrial diseases. Finding these proteins could help us gain valuable insight into pathophysiology of mitochondrial diseases. Recently, the combination of high-throughput omics techniques and complex bioinformatics analysis have brought new hope for revealing the pathogenesis and therapeutic targets about mitochondrial diseases. Increasingly, the quantitative proteomics and bioinformatics analysis can improve our understanding to the role of post-translational modifications[8]. Compared to data-dependent-acquisition (DDA) method, the use of data-independent acquisition (DIA) method can obtain more reliable results and require a smaller samples size. So, the DDA-based proteomics is gradually replaced by DIA-based proteomics. In recent years, as a new tool, DIA-based proteomics is increasingly applied to the study of various diseases[9].

In this study, we performed nanospray liquid chromatography-mass spectrometry (LC-MS) based proteomic analysis in the DIA modes on skeletal muscle specimens from patients with MELAS. The purpose of this study was to reveal the differentially expressed proteins in skeletal muscle tissue. Subsequently, we performed bioinformatics analysis for potential signaling pathways in the hope of gaining a better understanding of the pathogenesis.

2. Materials And Methods

2.1 Characteristics of individuals and muscle biopsy

The diagnostic criteria of MELAS study committee in Japan were adopted in this study[10].

Category A: Clinical findings of stroke-like episodes

1. headache with vomiting

2. seizure

3. hemiplegia

4. cortical blindness or hemianopsia

5. acute focal lesion observed via brain imaging

Category B: evidence of mitochondrial dysfunction including

1. high lactate levels (2 mmol/L or more) in plasma and/or cerebral spinal fluid or deficiency of mitochondrial-related enzyme activities

2. mitochondrial abnormalities in muscle biopsy

3. definitive gene mutation related to MELAS

Definitive MELAS

two items of Category A and two items of Category B (four items or more).

Suspicion of MELAS

one item of Category A and two items of Category B (at least three items).

In this study, all subjects underwent muscle biopsy for diagnostic purposes. We selected the MELAS patients positive point mutation for m.3243 A > G in genetic screening. We selected the age- and gender-matched subjects who were ultimately deemed to be free of neuromuscular diseases through muscle biopsies as controls. All collecting samples of muscle biopsies were informed consent of patients and controls. All procedures were approved by the Ethics committee of First Hospital of Shanxi Medical University (Taiyuan, China) and carried out in accordance with the principles of Helsinki Declaration.

2.2 Mitochondrial sequencing analysis

The entire mitochondrial genome was isolated and mitochondrial m.3243A > G mutation was detected by next-generation sequencing (NGS). Briefly, DNA was isolated from 200 mg muscle tissue by use of a DNA Kit CWE9600 (Beijing ComWin Biotech Co., Ltd), and mtDNA was amplified by long-range PCR using specific primer. Next-generation sequencing libraries were constructed by KAPA LTP Library Preparation Kit (KK8234, VWR, USA), and amplified libraries were used in Illumina NovaSeq High-throughput sequencing system (Illumina, USA). Sequenced data was assessed to be qualified by Sequencing Control Software (Illumina, USA) and analyzed by bioinformatic analysis referring human mitochondrial genome database. Mitochondrial m.3243A > G mutation was later confirmed by Sanger Sequencing using specific DNA primers flanking MT-TL1 gene.

2.3 Protein Digestion

100 µg of protein from each sample was solubilized in a new Eppendorf tube containing 8 M urea to achieve a final volume of 100 µL. Then, 2 µL of 0.5 M TCEP was added for incubation for 1 h at 37℃. After 40 minutes of incubation with 4 µL of 1 M iodoacetamide in the dark at room temperature, samples were then precipitated

by addition of -20℃ pre-chilled acetone at the ration of 1:5 at -20℃ overnight and centrifuged for 20 min at 12,000 G. Precipitates were washed and centrifuged again treated with 1 mL pre-chilled 90% acetone aqueous solution. Samples were re-dissolved in 100μL 100 mM TEAB and digested by Sequence grade modified trypsin (Promega, Madison, WI) containing 1:50 enzyme : protein (weight : weight) at 37℃ overnight. The peptide mixture was desalted by C18 ZipTip followed by quantification with Pierce™ Quantitative Colorimetric Peptide Assay (23275). SpeedVac was used for lyophilization.

2.4 Establish Spectrum Database

2.4.1 High PH reverse phase separation

The mixed peptides were re-dissolved in buffer A (buffer A: 20 mM ammonium formate in water, pH 10.0, adjusted with ammonium hydroxide) and then loaded onto a reverse phase column (XBridge C18 column, 4.6 mm x 250 mm, 5 μm, Waters Corporation, MA, USA) using Ultimate 3000 HPLC system (Thermo Fisher scientific, MA, USA). High pH separation was achieved in 40 min with a linear gradient starting from 5% B to 45% B (B: 20 mM ammonium formate in 80% ACN, pH 10.0, adjusted with ammonium hydroxide). The column was re-equilibrated at 30℃ for 15 min (flow rate: 1 mL/min). A total of 10 fractions were obtained and dried by vacuum concentrator for future use.

2.4.2 nano-HPLC-MS/MS Analysis

The peptides were re-dissolved in solvent A (A: 0.1% formic acid in water) and on-line nanospray LC-MS/MS was performed for analysis on an Orbitrap Lumos coupled to EASY-nLC 1200 system (Thermo Fisher Scientific, MA, USA). 4 μL peptide sample was loaded onto analytical column (Acclaim PepMap C18, 75 μm x 25 cm) and eluted with 120-min gradient from 4–32% B (B: 0.1% formic acid in ACN). We set the column flow rate at 300 nL/min and the capillary voltage at 2 kV. We run the mass spectrometer under DDA mode with MS and MS/MS mode automatically switched. The parameters were as follows: (1) MS: scan range (m/z) = 350–1500; resolution = 60,000; AGC target = 4e5; maximum injection time = 50 ms; dynamic exclusion = 30 s; (2) HCD-MS/MS: resolution = 15,000; AGC target = 5e4; maximum injection time = 38 ms; collision energy = 32.

2.4.3 Search the database

All Raw data were processed and analyzed by Spectronaut X (Biognosys AG, Switzerland) with default settings. Trypsin was assumed as the digestion enzyme with Spectronaut set up to search the database of swissprot_human_201902. The parameters were as follows: carbamidomethyl (C) was set as the fixed modification, while oxidation (M) was specified as the variable modifications. Q value (FDR) cutoff on precursor and protein level was set to 1%. Ultimately, an initial target list of 53,148 precursors, 37,666 peptides, 4,415 proteins and 4,301 protein group was obtained.

2.5 DIA-MS data processing

2.5.1 nano-HPLC-MS/MS Analysis

The samples were re-dissolved in 30 μL solvent A (A: 0.1% formic acid in water) from which 9μL was taken, added with 1μL 10 × iRT peptide, mixed, seperated with nano-LC, and finally analyzed by on-line nanospray LC-MS/MS on an Orbitrap Lumos coupled to EASY-nLC 1200 system (Thermo Fisher Scientific, MA, USA). 4 μL

peptide sample was loaded onto analytical column (Acclaim PepMap C18, 75 μm x 25 cm) and eluted with 120-min gradient from 4–32% B (B: 0.1% formic acid in ACN). We set the column flow rate at 300 nL/min and the capillary voltage at 2 kV. We run the mass spectrometer under DIA mode with MS and MS/MS mode automatically switched. The parameters were as follows: (1) MS: scan range (m/z) = 350–1350; resolution = 120,000; AGC target = 4e5; maximum injection time = 50 ms; (2) HCD-MS/MS: resolution = 30,000; AGC target = 1e6; collision energy = 32. (3) 60 variable Isolation windows was set with each window overlapped 1 m/z.

2.5.2 Data Analysis

We used Spectronaut X (Biognosys AG, Switzerland) with default settings to process and analyze the raw Data of DIA. Retention time prediction type was set to dynamic iRT and automatically determine the ideal extraction window. The criteria for protein identification were as follows: Q value (FDR) cutoff on precursor and protein level were both applied to 1%. The Decoy database was generated using a mutated strategy similar to scrambling a random number of amino acids (min = 2, max = length/2). All selected precursors that meet the screening conditions were used for quantification. All interfering fragment ions were excluded by MS2 interference unless less than 3 were found. The average value of the peak areas of the first 3 peptides less than 1.0% FDR was used to quantify the protein group. Different expressed proteins were filtered if their p value < 0.05 and fold change > 1.3 with Welch's ANOVA Test performed.

2.6 Bioinformatics Analysis

The partial least-squares-discriminant analysis (PLS-DA) is a classic PLS regression for solving discrimination and classification problems. Relevant analysis was performed by mixOmics package (https://CRAN.R-project.org/package=mixOmics). Hierarchical cluster analysis is an unsupervised method of clustering algorithms. The pheatmap package (https://CRAN.R-project.org/ package = pheatmap) was used in this analysis. The volcano plot is a kind of scatter-plot used to visualize changes in a data set within a given comparison. The X-axis and Y-axis represents the fold change and significance respectively. The ggplot2 package (http://ggplot2.org) was used in this study. Functional annotation was performed by Blast2GO version 5 and gene ontology (GO) analysis was performed using GOATOOLS[11, 12]. Kyoto Encyclopedia of Genes and Genomes (KEGG) pathway enrichment analysis was performed by KOBAS (http://kobas.cbi.pku.edu.cn/)[13]. The Protein-protein interaction (PPI) network was constructed using STRING v10 (www.string-db.org)[14].

3. Results

3.1 Clinical data

We recruited 10 patients (5 males, 5 females) with definitive MELAS from specialist clinics according to the diagnostic criteria in our hospital. The median age of the patients was 38.5 years (range 11–52). A tabulated description of clinical features of MELAS patients was shown in Table 1. The common symptoms were seizures and stroke. Other symptoms included headache, hearing loss, ataxia and weakness. The lactate levels was higher than 2 mmol/L in plasma at rest in 8 patients. The mutation heteroplasmy ranged from 56–89% in muscle tissue. These controls were healthy individuals without neuromuscular diseases and examined by the authors. A total of 10 controls (5 males, 5 females) with the median age of 39.5 years (range 12–53) were matched with patients for age and gender.

Table 1
Characteristics of the MELAS (mt 3243A > G) patients

No	Sex	Age	Onset of Age	Clinical symptoms	lactate level in plasma at rest	% muscle heteroplasmy	muscle biopsy	Head MRI
1	F	11	10	seizures, headache,	2.2 mmol/L	75	G(+), S(-)	left temporoparietal
2	M	47	42	myopathy	2.5 mmol/L	70	G(-),	lobes
3	F	26	23	hemiplegia, hearing loss,	4.5 mmol/L	83	S(+)	right occipital lobe and
4	F	45	40	impaired vision,	1.9 mmol/L	65	G(+), S(+)	left
5	M	52	49	diabetes, ataxia	1.8 mmol/L	56	G(+),	temporoparietal lobes
6	M	49	45	seizures,	3.1 mmol/L	70	S(+)	right temporal
7	M	31	30	headache, diabetes, short	3.4 mmol/L	79	S(+), C(+)	lobe
8	F	50	48	stature, hearing loss	4.3 mmol/L	80	G(-),	right occipital and temporal
9	F	32	30	diabetes,	3.3 mmol/L	80	S(+)	lobes
10	M	29	25	impaired vision, seizures, short stature	2.1 mmol/L	89	G(+), S(+)	bilateral temporal lobes
				blepharoptosis, seizures, hearing loss, hemiplegia, short stature			G(+), S(-)	left temporal and right occipital lobe
				seizures, headache, short stature, diabetes, impaired vision			G(+), S(-)	left temporal and occipital lobes
				headache, myopathy, hemiplegia, impaired vision, diabetes, short stature, ataxia			G(+), S(+)	left temporal lobe, right temporoparietal lobes
				seizures, hemiplegia, diabetes, short stature				left temporoparietal lobes, bilateral basal ganglia calcification
				headache, myopathy, seizures, ataxia,				bilateral temporoparietal lobes

G(+): ragged-red fiber (RRF) in MGT staining; S(+): strongly SDH-reactive blood vessels (SSV) or ragged-blue fibers (RBFs) in SDH staining; C(+): COX deficient fibers in COX staining

No	Sex	Age	Onset of Age	Clinical symptoms	lactate level in plasma at rest	% muscle heteroplasmy	muscle biopsy	Head MRI
				impaired glucose tolerance, short stature blepharoptosis, myopathy, ataxia, seizures, headache, hearing loss				
G(+): ragged-red fiber (RRF) in MGT staining; S(+): strongly SDH-reactive blood vessels (SSV) or ragged-blue fibers (RBFs) in SDH staining; C(+): COX deficient fibers in COX staining								

3.2 Muscle biopsy

The patients: multiple RRFs were found upon HE (Fig. 1A) and MGT staining (Fig. 1B). Some fibers exhibited elevated levels of succinate dehydrogenase even ragged blue fibers (RBFs) were found upon SDH staining (Fig. 1C). SDH/COX double staining revealed that SDH was strongly positive of COX negative/decreased fibers (Fig. 1D). There were unremarkable findings upon ATP staining, oil red O (ORO) staining and periodic acid-schiff (PAS) staining.

The controls: no obvious abnormality were found in the muscle biopsy upon HE, MGT, SDH, COX, ATP, PAS and ORO staining.

3.3 Mutational analysis

The mitochondrial m.3243A > G mutation was found by NGS and later confirmed by conventional Sanger Sequencing in MELAS patients (Fig. 2a). This mutation was absent in the controls by Sanger Sequencing (Fig. 2b).

3.4 Identification of the differences between MELAS and controls

The PLS-DA model showed obvious difference, indicating a good class difference between the two groups (Fig. 3). The Volcano plots of differential proteins revealed 128 differential proteins (Supplementary 1) were ultimately obtained between MELAS and controls, including 68 down-regulated proteins and 60 up-regulated proteins (Fig. 4). Heat map analysis exhibited levels of differential proteins in every samples and provided information on the underlying metabolic disorders caused by m.3243A > G in muscle (Fig. 5). These results suggested that although donor variation existed, the differential proteins were generally MELAS-relevant.

3.4.1 Proteins signature of glycometabolism

We studied the expression of proteins involved in glycogen synthesis (Glycogenin-1, GYG1), glycolysis (glyceraldehyde-3-phosphate dehydrogenase, GAPDH; enolase 1, ENO1 and lactate dehydrogenase A, LDHA)

and glycogenolysis (muscle isoform of glycogen phosphorylase, PYGM). The GYG1 expression was significantly increased in MELAS patients compared with controls. Interestingly, there were no differences in the other proteins signature between the two groups in Table 2.

Table 2
The protein signature of glycometabolism

Protein ID	Protein	Protein descriptions	Genes	Fold Change Ratio	P Value
P00558	PGK1	Phosphoglycerate kinase 1	PGK1	1.010862	0.909051
P06733	ENOA	Alpha-enolase	ENO1	1.052366	0.67941
P04406	G3P	Glyceraldehyde-3-phosphate dehydrogenase	GAPDH	0.947695	0.679475
P00338	LDHA	L-lactate dehydrogenase A chain	LDHA	0.984829	0.945883
P21695	GPDA	Glycerol-3-phosphate dehydrogenase [NAD(+)], cytoplasmic	GPD1	1.09059	0.560181
P46976	GLYG	Glycogenin-1	GYG1	1.300340247	0.007447

3.4.2 The mitochondrial structural proteins

Subsequently, we analyzed the differences in Hsp60 (a mitochondrial structural protein) and mitochondrial inner membrane protein (calcium uptake protein 2, MICU2 and choline dehydrogenase, CHDH). We also focused on the expression of the enzymes related to the decarboxylation of pyruvate (pyruvate dehydrogenase, PDH-E1α), tricarboxylic acid cycle (citrate synthase, CS), oxidation of fatty acids (hydroxyacyl-CoA dehydrogenase/3-ketoacyl-CoA thiolase/enoyl-CoA hydratase, alpha subunit, HADHA) and mitochondrial translation (pentatricopeptide repeat domain-containing protein 3, PTCD3). No differences in expression of Hsp60, PDH-E1α and CS were observed between the two groups (Table 3). Interestingly, the expression of HADHA was increased but CHDH was decreased when compared to controls. The GYG1 expression was significantly increased in MELAS patients. The PTCD3 and MICU2 were not expressed at all in MELAS patients (Table 3).

Table 3
The protein signature of mitochondrial structure

Protein ID	Protein	Protein descriptions	Genes	Fold Change Ratio	P Value
P10809	CH60	60 kDa heat shock protein	HSPD1	0.943623	0.65031
P08559	ODPA	Pyruvate dehydrogenase E1 component subunit alpha	PDHA1	0.905403	0.343616
O75390	CISY	Citrate synthase	CS	0.920595	0.532728
P40939	ECHA	Trifunctional enzyme subunit alpha	HADHA	1.238323	0.018426
Q8IYU8	MICU2	Calcium uptake protein 2	MICU2	0	0.000001
Q96EY7	PTCD3	Pentatricopeptide repeat domain-containing protein 3	PTCD3	0	0.000001
Q8NE62	CHDH	Choline dehydrogenase	CHDH	0.329519729	0.028366

3.4.3 Proteins involved in the oxidative stress and antioxidant defense

Finally, we analyzed the differences in proteins involved in oxidative stress: glucose-6-phosphate dehydrogenase (G6PD), selenoprotein P (SEPP1), heat shock protein beta-1 (HSPB1), alpha-crystallin B chain (CRYAB) and heme oxygenase 1 (HMOX1). At the same time, we focused on the differences in proteins associated with antioxidant defense: superoxide dismutase 1 (SOD1), superoxide dismutase 2 (SOD2) and protein S100-A9 (S100A9). The results indicated that the G6PD expression in the skeletal muscle was obviously reduced in MELAS patients. The SEPP1 was not expressed at all in MELAS patients. On the contrary, the expression of HSPB1 and CRYAB were obviously up-regulated in patients. The S100A9 was up-regulated in patients when compared to controls. The HMOX1 was not expressed at all in controls. There were no differences in the expression of SOD1 and SOD2 between the two groups (Table 4).

Table 4
The protein signature of oxidative stress and antioxidant defense

Protein ID	Protein	Protein descriptions	Genes	Fold Change Ratio	P Value
P11413	G6PD	Glucose-6-phosphate 1-dehydrogenase	G6PD	0.143321113	0.031176
P49908	SEPP1	Selenoprotein P	SELENOP	0	0.000001
P04792	HSPB1	Heat shock protein beta-1	HSPB1	1.489312	0.0105384
P02511	CRYAB	Alpha-crystallin B chain	CRYAB	1.376931	0.0228972
P09601	HMOX1	Heme oxygenase 1	HMOX1	-	0.000001
P00441	SODC	Superoxide dismutase [Cu-Zn]	SOD1	1.014766	0.940828
P04179	SODM	Superoxide dismutase [Mn]	SOD2	1.24379	0.546555
P06702	S10A9	Protein S100-A9	S100A9	1.311881	0.04811

3.5 Gene ontology (GO) analysis

The 128 identified differential proteins in the two groups were categorized into three groups: CC, MF and BP. The intracellular part, membrane-bounded organelle and extracellular organelle were the three most enriched CC (Fig. 6A). The results indicated that protein binding, iron binding and lipid binding were the three most enriched MF (Fig. 6B). The response to stress, response to chemical, response to external stimulus, immune response and interspecies interaction between organisms were the most enriched BP (Fig. 6C).

3.6 KEGG pathway enrichment and PPI network analysis

We performed KEGG pathway enrichment analysis to deepen the understanding to the functions of the differential proteins. We observed that these pathways, including hematopoietic cell lineage, Epstein-Barr virus infection, phagosome, systemic lupus erythematosus, proliferator-activated receptors (PPAR) signaling pathway, ribosome, viral myocarditis and vitamin B6 metabolism showed significant enrichment (Fig. 7). We constructed PPI networks by using the STRING database to help us better understand the interactions of differential proteins. A total of 128 proteins were used as search inputs, 93 of which were matched in the database, including 43 up-regulated proteins and 50 down-regulated proteins. The PPI network of differential proteins was performed as shown in Figs. 8 and 11 key proteins were discovered in the PPI network analysis, with HSPB1 as the most important, which connected 8 nodes. There were 4 proteins including G6PD, HMOX1, SNRPB, MRPL22, connecting 5 nodes. The remaining 6 proteins (STMN1, MMP2, UGDH, CD14, MRPL4 and MRPL18) connected 4 nodes. HSPB1, HMOX1, CD14, MRPL22 and MRPL18 in the module were up-regulated and G6PD, SNRPB, STMN1, MMP2, UGDH and MRPL4 were down-regulated.

4. Discussion

So far, this is the first proteomes analysis of skeletal muscle collected from m.3243A > G MELAS patients compared with controls using the method of the DIA. We had found 128 differential proteins, including 68 proteins for down-regulation and 60 proteins for up-regulation. We studied the expression involved in oxidative stress and found a highly significant up-regulation including HSPB1, CRYAB, HMOX1 but a decrease in G6PD and SEPP1. The most key proteins were HSPB1 and CRYAB, which were small heat shock proteins (sHsp) that combined misfolded proteins to prevent them from denaturation, inhibited cellular apoptosis and regulated the intracellular redox state as molecular chaperones[15, 16]. In mutant HSPB1 expressing motor axons, the researchers observed the decreased mitochondrial Complex I activity and increased mitochondrial vulnerability, resulted in increased superoxide release and decreased mitochondrial glutathione levels[17]. The CRYAB could protect cells from hypoxia and maintain mitochondrial integrity[18, 19] and also had other roles in vascular biology[20]. The CRYAB was crucial for endothelial cell survival in hypoxia[19, 21, 22]. sHsps could attenuate mitochondrial dysfunctions, block oxidative stress and minimize neuronal apoptosis, so sHsps were promising protectants in some neurodegenerative diseases[23]. G6PD was the first rate-limiting enzyme in the pentose phosphate pathway which was necessary to maintain oxidation-reduction equilibrium in cells[24]. There were some studies found that sHsp significantly increased G6PD activity and played the role of anti-oxidative stress through a G6PD-dependent ability[16]. Our results showed that G6PD was down-regulated, different from another study[25]. We considered that there were some reasons: firstly, the pathogenesis of MELAS was extremely complex; secondly, the muscle tissue only provided the fleeting information about a certain stage in the course

of MELAS; thirdly, sHsps played the anti-oxidative stress role through other pathways rather than regulating G6PD-dependent ability. In our study, the HMOX1 was highly significant up-regulation in MELAS but not expression at all in controls. The HMOX-1 over-expression associated with intracellular oxidative stress, mitochondrial dysfunction and mitophagy[26]. Increased levels of HMOX1 had been observed in many neurodegenerative diseases including Alzheimer's, Parkinson's diseases[26]. Thus, we speculated that these oxidative-related proteins might be associated to the development and severity of clinical symptoms of MELAS.

We had discovered these pathways, including phagosome, PPAR signaling pathway, ribosome and vitamin B6 metabolism showed significant enrichment. There was a study that the authors had found accumulation of autophagosomes in MELAS fibroblasts[27]. The enhancement of autophagosome content might be an adaptive response to intracellular OXPHOS and mitochondrial deficiency. As compensatory response, the increased antophagosome could clear damaged mitochondria to avoid further cellular dysfunction[28, 29]. On the contrary, the mitochondrial dysfunction blocked both autophagy induction and autophagic flux[30]. So it was controversial whether autophagy played protective or harmful effects. Defects in phagosome was related to a variety of cellular metabolic process, including abnormal lipid metabolism, oxidative stress injure and mitochondrial dysfunction[31–33] but autophagosome accumulation could impair cell bioenergetics and also induce cell death[34]. We proposed that the response to autophagosome varied widely, depending on the severity of mitochondrial deficiency. The phagosome pathway may be one of the improtant molecular networks involved in the pathogenesis of MELAS.

PPAR signaling pathway is a crucial regulator for the β oxidation of fatty acid[35, 36] and promote transcription of nuclear-encoded mitochondrial genes. Bezafibrate, as a pan-PPAR activator, could up-regulate the expression of Peroxisome proliferator-activated receptor gamma coactivator 1-alpha (PGC-1α), which promoted mitochondrial biogenesis and improved mitochondrial deficiency of mitochondrial diseases[37]. The PPAR signaling pathway may be a potentially disease-modifying therapeutic target.

The mitochondrial ribosome proteins (MRPs) were synthesized in the cytoplasm, introduced into mitochondria for assembly and then responsible for the translation of 13 mitochondrial mRNAs[38]. In our study, MRPL22, MRPL18 were up-regulated and MRPL4, PTCD3 were down-regulated. MRPL18 facilitates ribosome assembly to participate in selected mRNAs translation and stress regulation to achieve a strong cytoplasmic stress response under stress conditions[39]. So MRPL18 is one of a key regulator to cytoplasmic stress response. PTCD3, also known as MRPS39, is one of the mitochondrial ribosomal supernumerary proteins unique to mammals[40]. A study of PTCD3 knockdown showed protein synthesis was seriously disturbed to result in OXPHOS deficiency, although no effect on RNA metabolism[41]. PTCD3 mutations led to impaired translation of mtDNA-encoded proteins, resulting in combined defects of Complex I and IV, and decreased ATP production[42]. Although MRPL4 had not been reported in the mitochondrial diseases, this molecule had attracted increasing attention from researchers because it had been reported to be downstream of hypoxia-inducible factor-1α (HIF-1α)[43]. From the above, we speculated that the MRPs played a key role in the occurrence, development and prognosis of MELAS.

Of course, this study also had certain limitations: first of all, limited by the sample size, the results could not accurately reflect the complete picture of MELAS. The Second, we tried to minimize the individual differences, but the skeletal muscle only provided fleeting information about a certain stage in the MELAS process. The third, the DIA protein library was established on the basis of the DDA atlas database and the might lead to the loss of some peptides in the process of analysis. Therefore, the larger sample size and more quantitative studies were needed to verify our results.

5. Conclusion

Our results indicated that a large number of differential proteins were repeatedly recognized in skeletal muscle of MELAS patients. In addition, the results revealed that the imbalance between oxidative stress and antioxidant defense, activation of autophagosomes and abnormal metabolism of mitochondrial ribosome proteins played a critical role in m.3243A > G MELAS patients. Finally, further investigation of these proteins could contribute novel insights to the pathogenesis of MELAS in a comprehensive manner.

Declarations

Ethics approval and consent to participate

All collecting samples of muscle biopsies were informed consent of patients and controls. All procedures were approved by the Ethics committee of First Hospital of Shanxi Medical University (Taiyuan, China) and carried out in accordance with the principles of Helsinki Declaration.

Competing interests

The authors have no conflicts of interest to report.

Availability of data and material

The datasets used or analysed during the current study are available from the corresponding author on reasonable request.

Funding

We thank the Key Research and Development (R&D) Projects of Shanxi Province (No. 201603D321081), the Natural Science Foundation for Young Scientists of Shanxi Province (No. 201801D221415) and Shanxi Medical University Postdoctoral Startup Fund (No. 032308) for the costs of samples collection and MS testing.

Authors' contributions

Junhong Guo and Hui Zhang raised and designed this subject. Xueli Chang collected and extracted data, and drafted the article. Xueli Chang, Wei Zhang and Li Yan analyzed the data. Chuanqiang Pu and Qiang Shi

provided some muscle tissue samples. Juan Wang, Jing Zhang and Wenqu Yang interpreted the results and revised the manuscript.

Consent for publication

All authors read and approved the final version of this manuscript for submission.

Acknowledgments

We thank all participants and their families who have performed the muscle biopsy. We also thank the omicsolution company in Shanghai for providing technical support.

References

1. Schaefer AM, McFarland R, Blakely EL, He L, Whittaker RG, Taylor RW, et al. Prevalence of mitochondrial DNA disease in adults. Ann Neurol. 2008;63:35–9.
2. Gorman GS, Schaefer AM, Ng Y, Gomez N, Blakely EL, Alston CL, et al. Prevalence of nuclear and mitochondrial DNA mutations related to adult mitochondrial disease. Ann Neurol. 2015;77:753–9.
3. Pavlakis SG, Phillips PC, DiMauro S, De Vivo DC, Rowland LP. Mitochondrial myopathy, encephalopathy, lactic acidosis, and strokelike episodes: A distinctive clinical syndrome. Ann Neurol. 1984;16:481–8.
4. Zhang J, Guo J, Fang W, Jun Q, Shi K. Clinical features of melas and its relation with a3243g gene point mutation. Int J Clin Exp Pathol. 2015;8:13411–5.
5. Limongelli G, Tome-Esteban M, Dejthevaporn C, Rahman S, Hanna MG, Elliott PM. Prevalence and natural history of heart disease in adults with primary mitochondrial respiratory chain disease. Eur J Heart Fail. 2010;12:114–21.
6. Esterhuizen K, Lindeque JZ, Mason S, van der Westhuizen FH, Suomalainen A, Hakonen AH, et al. A urinary biosignature for mitochondrial myopathy, encephalopathy, lactic acidosis and stroke like episodes (melas). Mitochondrion. 2019;45:38–45.
7. Calvo SE, Clauser KR, Mootha VK. Mitocarta2.0: An updated inventory of mammalian mitochondrial proteins. Nucleic acids research. 2016;44:D1251–7.
8. Wang W, Karamanlidis G, Tian R. Novel targets for mitochondrial medicine. Science translational medicine. 2016;8:326rv323.
9. Chapman JD, Goodlett DR, Masselon CD. Multiplexed and data-independent tandem mass spectrometry for global proteome profiling. Mass spectrometry reviews. 2014;33:452–70.
10. Yatsuga S, Povalko N, Nishioka J, Katayama K, Kakimoto N, Matsuishi T, et al. Melas: A nationwide prospective cohort study of 96 patients in japan. Biochim Biophys Acta. 2012;1820:619–24.
11. Conesa A, Gotz S, Garcia-Gomez JM, Terol J, Talon M, Robles M. Blast2go: A universal tool for annotation, visualization and analysis in functional genomics research. Bioinformatics. 2005;21:3674–6.
12. Klopfenstein DV, Zhang L, Pedersen BS, Ramirez F, Warwick Vesztrocy A, Naldi A, et al. Goatools: A python library for gene ontology analyses. Scientific reports. 2018;8:10872.

13. Xie C, Mao X, Huang J, Ding Y, Wu J, Dong S, et al. Kobas 2.0: A web server for annotation and identification of enriched pathways and diseases. Nucleic acids research. 2011;39:W316–22.
14. Szklarczyk D, Franceschini A, Wyder S, Forslund K, Heller D, Huerta-Cepas J, et al. String v10: Protein-protein interaction networks, integrated over the tree of life. Nucleic acids research. 2015;43:D447–52.
15. Mehlen P, Kretz-Remy C, Preville X, Arrigo AP. Human hsp27, drosophila hsp27 and human alphab-crystallin expression-mediated increase in glutathione is essential for the protective activity of these proteins against tnfalpha-induced cell death. EMBO J. 1996;15:2695–706.
16. Preville X, Salvemini F, Giraud S, Chaufour S, Paul C, Stepien G, et al. Mammalian small stress proteins protect against oxidative stress through their ability to increase glucose-6-phosphate dehydrogenase activity and by maintaining optimal cellular detoxifying machinery. Experimental cell research. 1999;247:61–78.
17. Kalmar B, Innes A, Wanisch K, Kolaszynska AK, Pandraud A, Kelly G, et al. Mitochondrial deficits and abnormal mitochondrial retrograde axonal transport play a role in the pathogenesis of mutant hsp27-induced charcot marie tooth disease. Human molecular genetics. 2017;26:3313–26.
18. Diokmetzidou A, Soumaka E, Kloukina I, Tsikitis M, Makridakis M, Varela A, et al. Desmin and alphab-crystallin interplay in the maintenance of mitochondrial homeostasis and cardiomyocyte survival. Journal of cell science. 2016;129:3705–20.
19. Kannan R, Sreekumar PG, Hinton DR. Alpha crystallins in the retinal pigment epithelium and implications for the pathogenesis and treatment of age-related macular degeneration. Biochim Biophys Acta. 2016;1860:258–68.
20. Sinha D, Klise A, Sergeev Y, Hose S, Bhutto IA, Hackler L Jr, et al. Betaa3/a1-crystallin in astroglial cells regulates retinal vascular remodeling during development. Mol Cell Neurosci. 2008;37:85–95.
21. Kase S, He S, Sonoda S, Kitamura M, Spee C, Wawrousek E, et al. Alphab-crystallin regulation of angiogenesis by modulation of vegf. Blood. 2010;115:3398–406.
22. Kannan R, Sreekumar PG, Hinton DR. Novel roles for alpha-crystallins in retinal function and disease. Prog Retin Eye Res. 2012;31:576–604.
23. Zhu Z, Reiser G. The small heat shock proteins, especially hspb4 and hspb5 are promising protectants in neurodegenerative diseases. Neurochem Int. 2018;115:69–79.
24. Puthumana JS, Regenold WT. Glucose-6-phosphate dehydrogenase activity in bipolar disorder and schizophrenia: Relationship to mitochondrial impairment. J Psychiatr Res. 2019;112:99–103.
25. Santacatterina F, Torresano L, Nunez-Salgado A, Esparza-Molto PB, Olive M, Gallardo E, et al. Different mitochondrial genetic defects exhibit the same protein signature of metabolism in skeletal muscle of peo and melas patients: A role for oxidative stress. Free Radic Biol Med. 2018;126:235–48.
26. Schipper HM, Song W, Tavitian A, Cressatti M. The sinister face of heme oxygenase-1 in brain aging and disease. Progress in neurobiology. 2019;172:40–70.
27. Cotan D, Cordero MD, Garrido-Maraver J, Oropesa-Avila M, Rodriguez-Hernandez A, Gomez Izquierdo L, et al. Secondary coenzyme q10 deficiency triggers mitochondria degradation by mitophagy in melas fibroblasts. FASEB journal: official publication of the Federation of American Societies for Experimental Biology. 2011;25:2669–87.

28. Rodriguez-Hernandez A, Cordero MD, Salviati L, Artuch R, Pineda M, Briones P, et al. Coenzyme q deficiency triggers mitochondria degradation by mitophagy. Autophagy. 2009;5:19–32.
29. Moran M, Delmiro A, Blazquez A, Ugalde C, Arenas J, Martin MA. Bulk autophagy, but not mitophagy, is increased in cellular model of mitochondrial disease. Biochim Biophys Acta. 2014;1842:1059–70.
30. Graef M, Nunnari J. Mitochondria regulate autophagy by conserved signalling pathways. EMBO J. 2011;30:2101–14.
31. Jiang M, Esteve-Rudd J, Lopes VS, Diemer T, Lillo C, Rump A, et al. Microtubule motors transport phagosomes in the rpe, and lack of klc1 leads to amd-like pathogenesis. J Cell Biol. 2015;210:595–611.
32. Reyes-Reveles J, Dhingra A, Alexander D, Bragin A, Philp NJ, Boesze-Battaglia K. Phagocytosis-dependent ketogenesis in retinal pigment epithelium. J Biol Chem. 2017;292:8038–47.
33. Toms M, Burgoyne T, Tracey-White D, Richardson R, Dubis AM, Webster AR, et al. Phagosomal and mitochondrial alterations in rpe may contribute to kcnj13 retinopathy. Scientific reports. 2019;9:3793.
34. Debnath J, Baehrecke EH, Kroemer G. Does autophagy contribute to cell death? Autophagy. 2005;1:66–74.
35. Kersten S, Stienstra R. The role and regulation of the peroxisome proliferator activated receptor alpha in human liver. Biochimie. 2017;136:75–84.
36. Scarpulla RC. Transcriptional paradigms in mammalian mitochondrial biogenesis and function. Physiological reviews. 2008;88:611–38.
37. Bastin J, Aubey F, Rotig A, Munnich A, Djouadi F. Activation of peroxisome proliferator-activated receptor pathway stimulates the mitochondrial respiratory chain and can correct deficiencies in patients' cells lacking its components. J Clin Endocrinol Metab. 2008;93:1433–41.
38. Christian BE, Spremulli LL. Mechanism of protein biosynthesis in mammalian mitochondria. Biochim Biophys Acta. 2012;1819:1035–54.
39. Zhang X, Gao X, Coots RA, Conn CS, Liu B, Qian SB. Translational control of the cytosolic stress response by mitochondrial ribosomal protein l18. Nat Struct Mol Biol. 2015;22:404–10.
40. Filipovska A, Rackham O. Pentatricopeptide repeats: Modular blocks for building rna-binding proteins. RNA Biol. 2013;10:1426–32.
41. Davies SM, Rackham O, Shearwood AM, Hamilton KL, Narsai R, Whelan J, et al. Pentatricopeptide repeat domain protein 3 associates with the mitochondrial small ribosomal subunit and regulates translation. FEBS Lett. 2009;583:1853–8.
42. Borna NN, Kishita Y, Kohda M, Lim SC, Shimura M, Wu Y, et al. Mitochondrial ribosomal protein ptcd3 mutations cause oxidative phosphorylation defects with leigh syndrome. Neurogenetics. 2019;20:9–25.
43. Benita Y, Kikuchi H, Smith AD, Zhang MQ, Chung DC, Xavier RJ. An integrative genomics approach identifies hypoxia inducible factor-1 (hif-1)-target genes that form the core response to hypoxia. Nucleic acids research. 2009;37:4587–602.

Figures

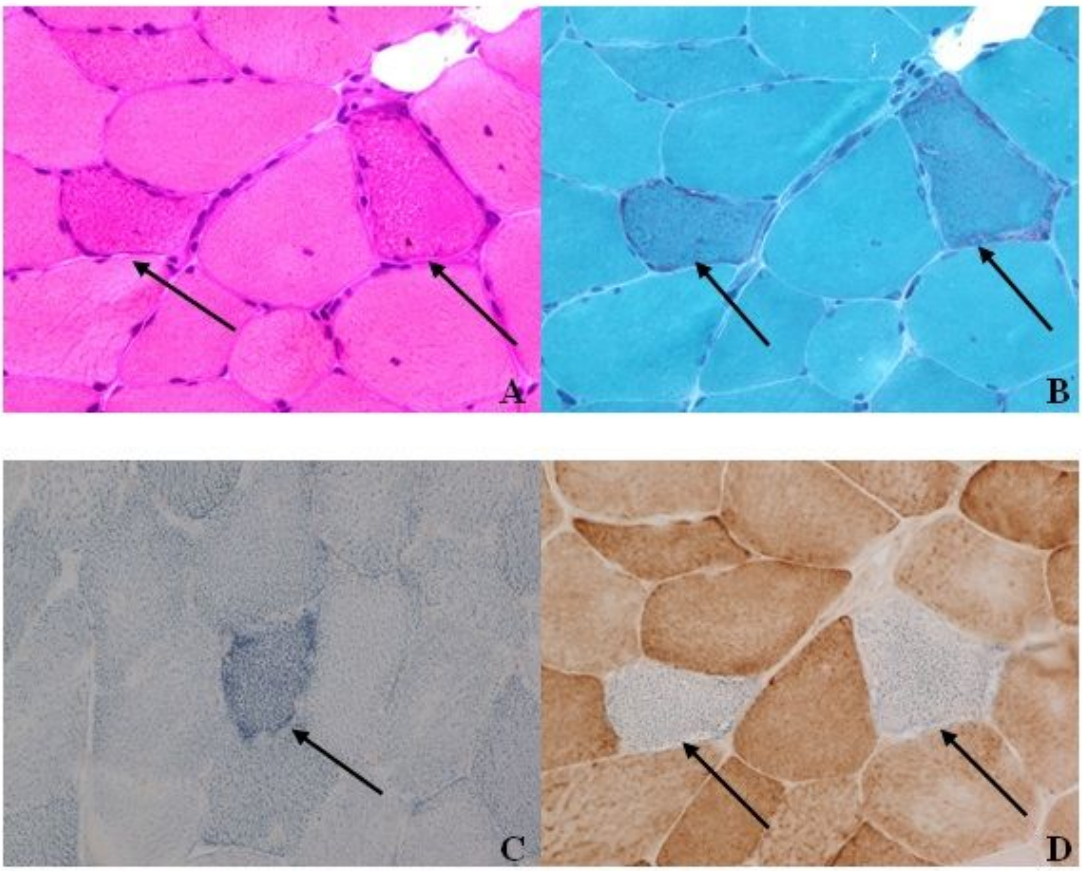

Figure 1

Mitochondrial abnormalities in muscle biopsy of patients A: H&E staining reveals ragged-red fibers (RRFs). B: MGT staining also reveals RRFs. C: SDH staining reveals ragged-blue fibers (RBFs). D: SDH/COX double staining reveals that SDH was strongly positive of COX negative/decreased fibers.

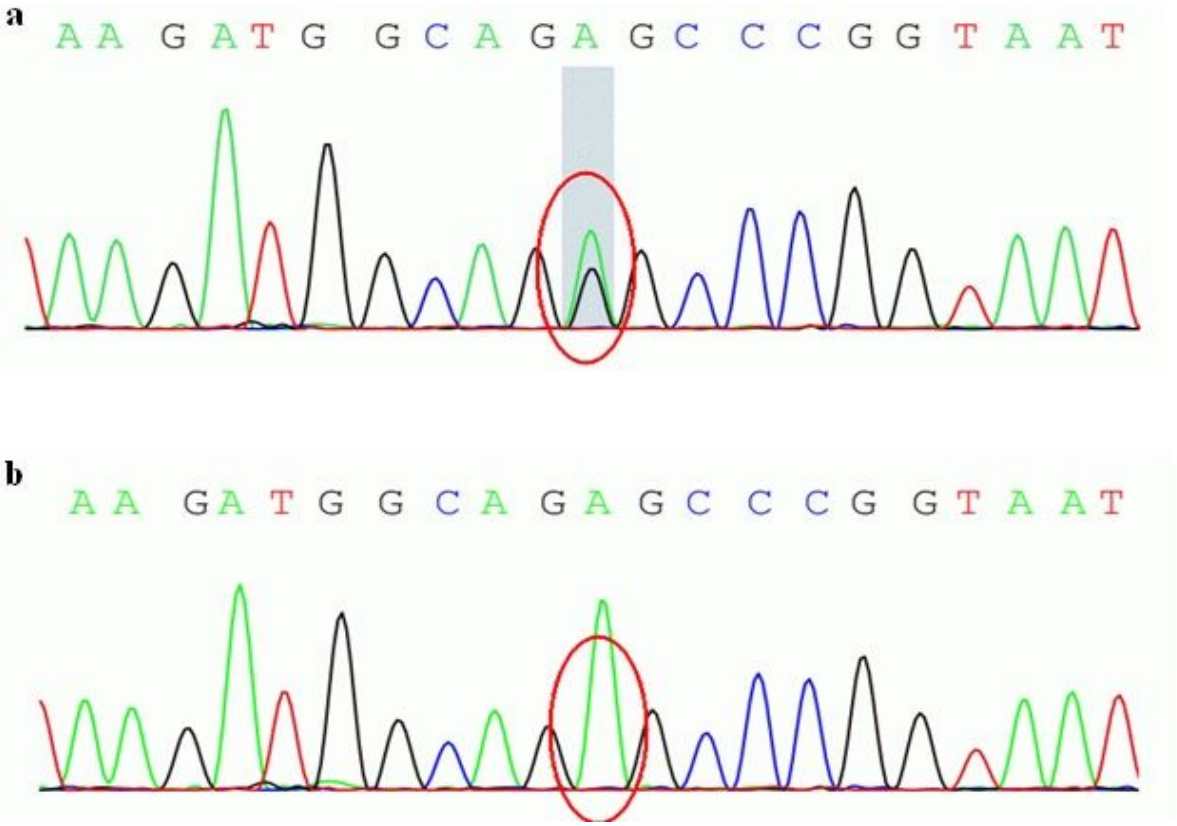

Figure 2

Results of mitochondrial m.3243A>G mutation by Sanger Sequencing a: the m.3243G>A mutation postive in MELAS patients b: the m.3243A>G mutation negative in control

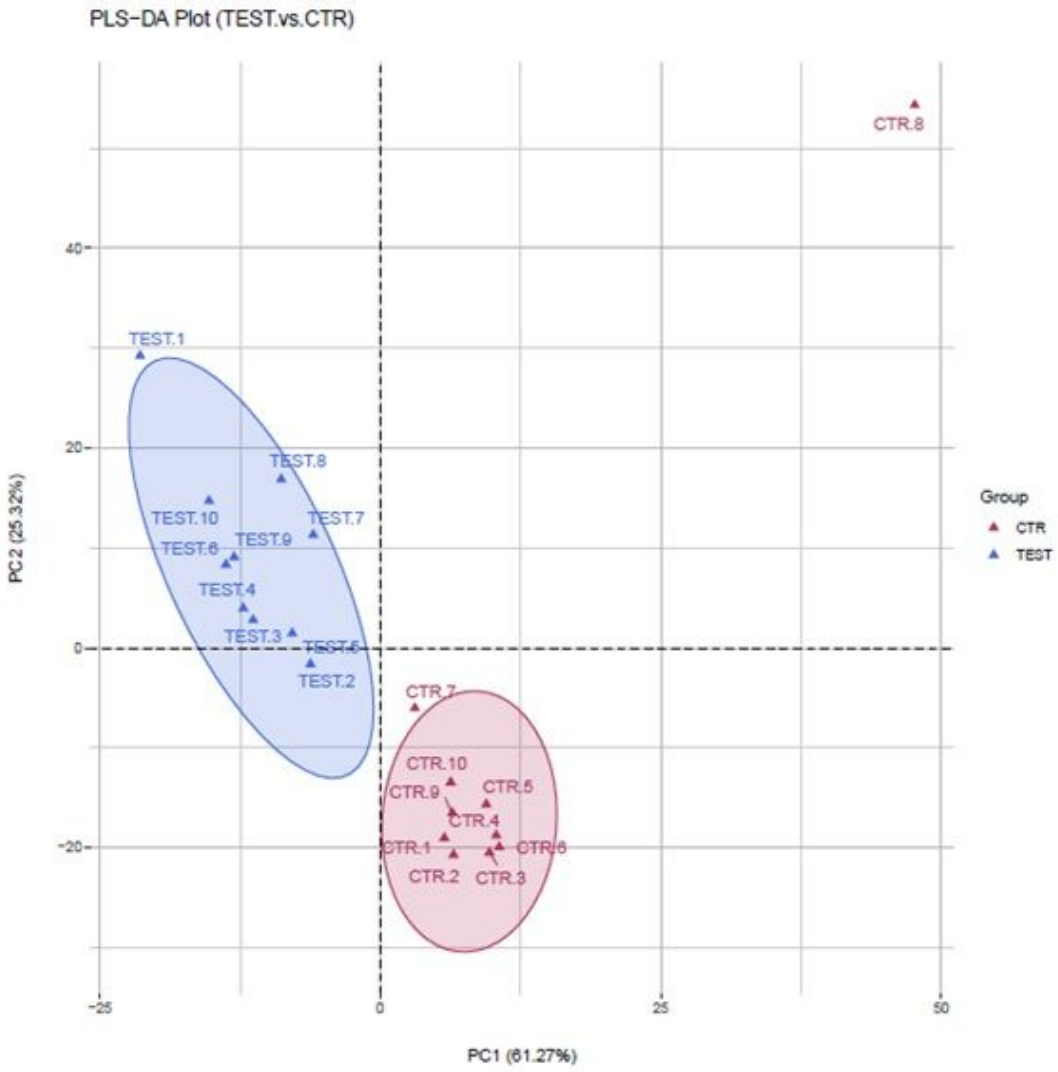

Figure 3

The PLS-DA model of the MELAS and Control groups All observed MS peaks are included in the model; Clear separation of the groups is observed, showing distinct class membership. TEST: MELAS patients; CTR: control

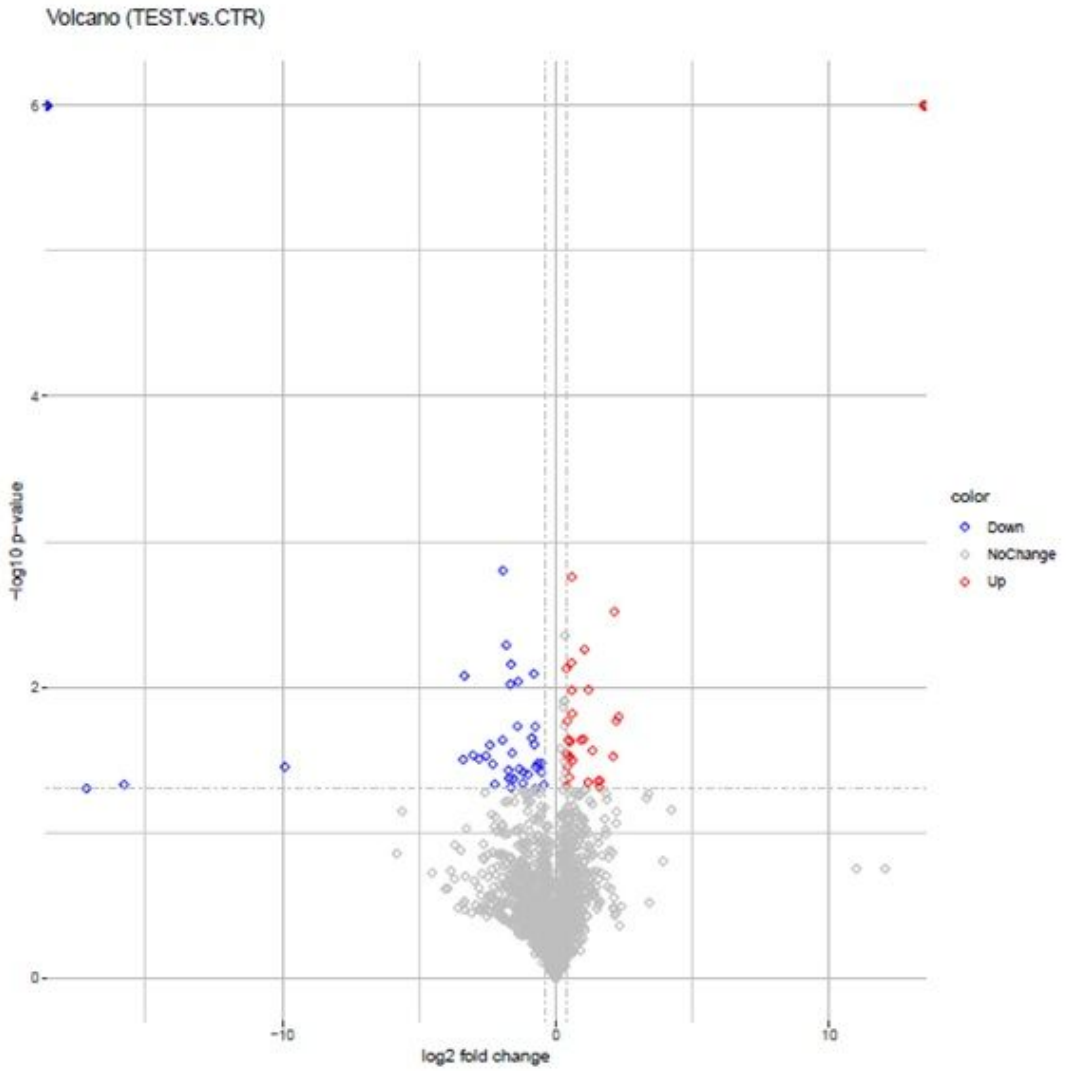

Figure 4

Volcano plots of differential proteins between MELAS and control Data points in red represent up-regulated and green represent down-regulated proteins. Proteins without any significant difference are in gray. TEST: MELAS patients; CTR: control

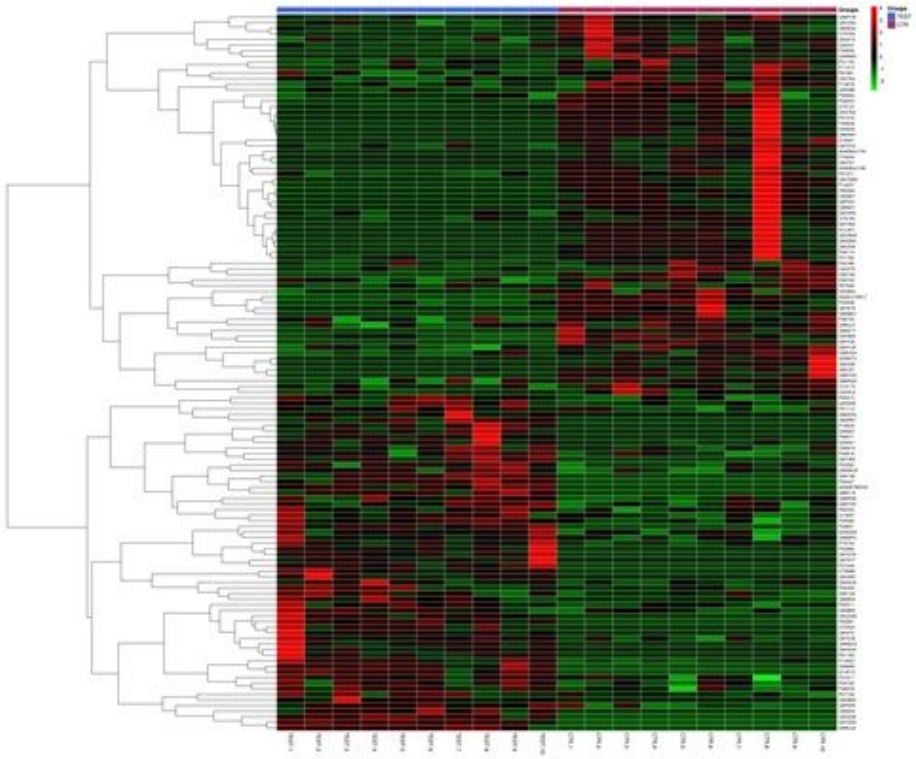

Figure 5

The heat map of differential proteins in muscle sample between MELAS and control groups Each line means a protein, and each column id for each sample. TEST.1−TEST.10 represent replicates in the MELAS group and CTR.1−CTR.10, in the control group. The up-regulated proteins are shown in red color, whereas the down-regulated proteins are presented in green color.

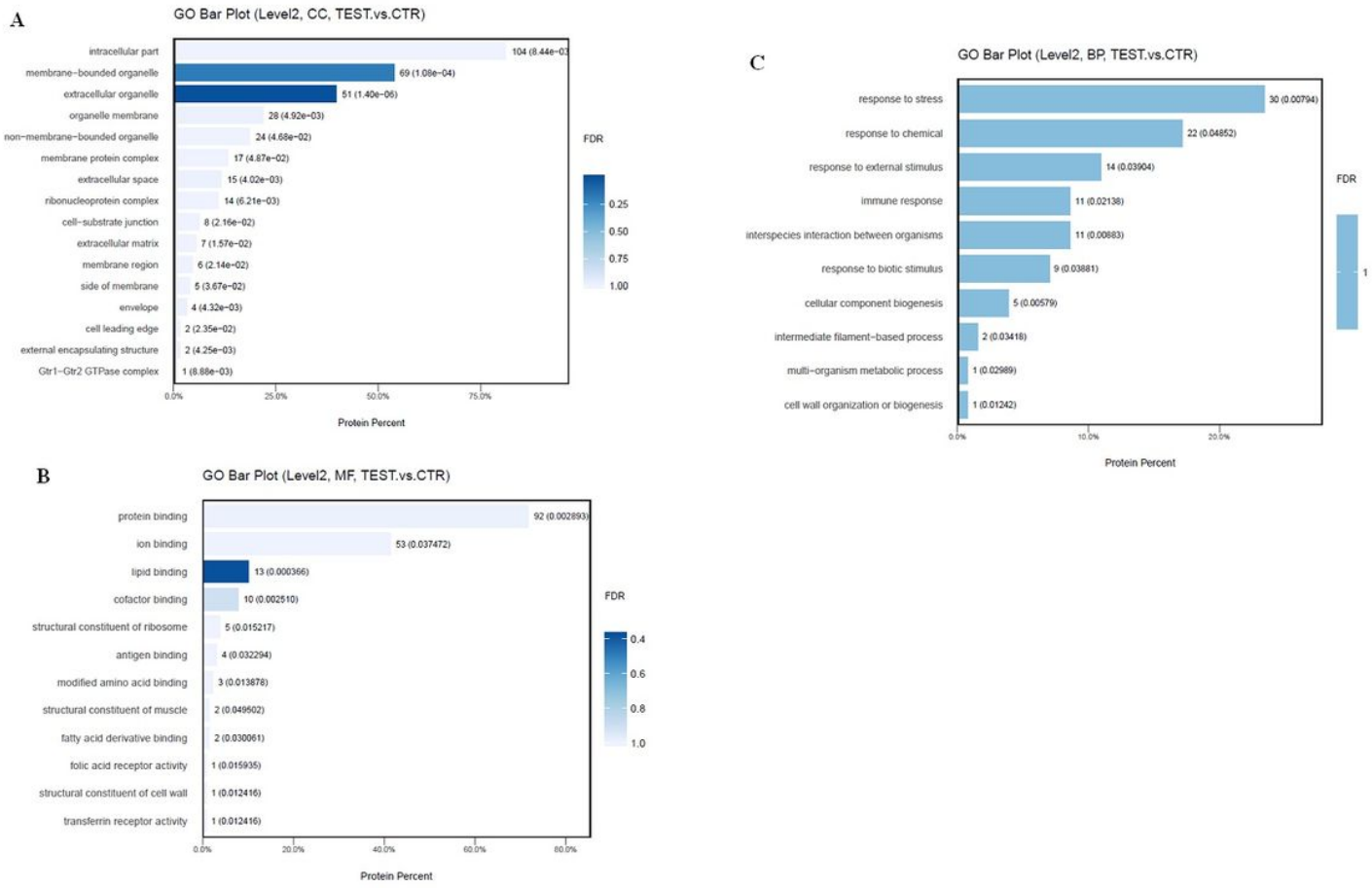

Figure 6

GO analysis of the differential proteins in the two groups A: cellular components, B: molecular functions, C: biological process. False discovery rate (FDR) of GO analysis was acquired from functional annotation tool. p <0.05. TEST: MELAS patients; CTR: control

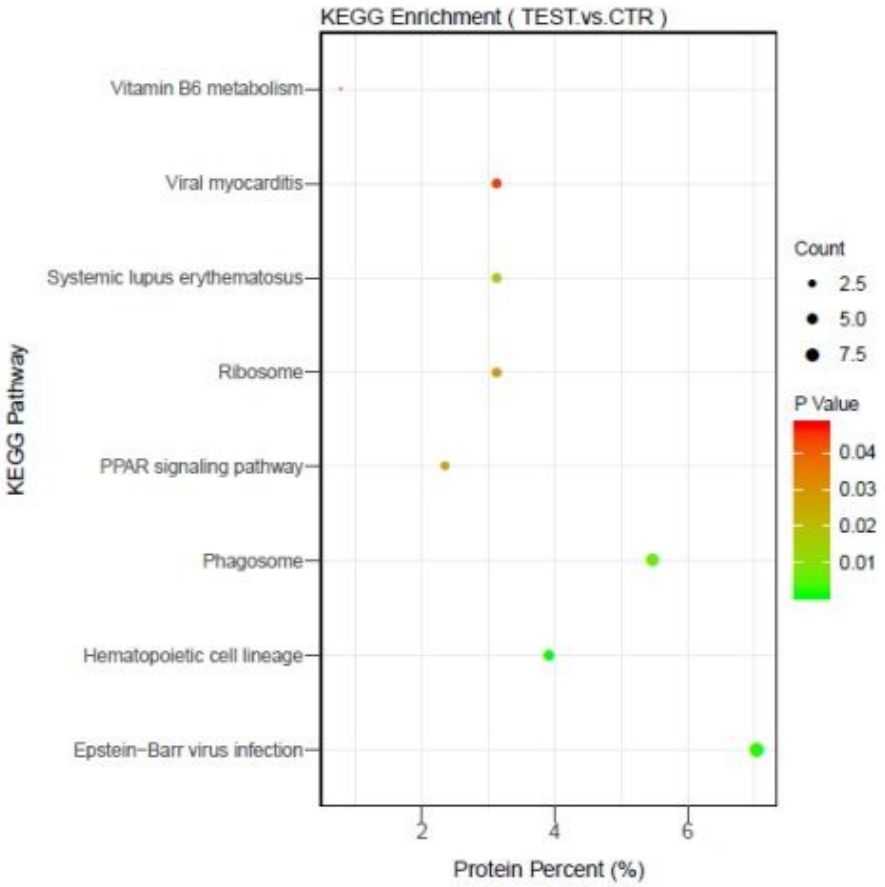

Figure 7

KEGG pathway enrichment analysis based on the identified proteins in MELAS and control TEST: MELAS patients; CTR: control

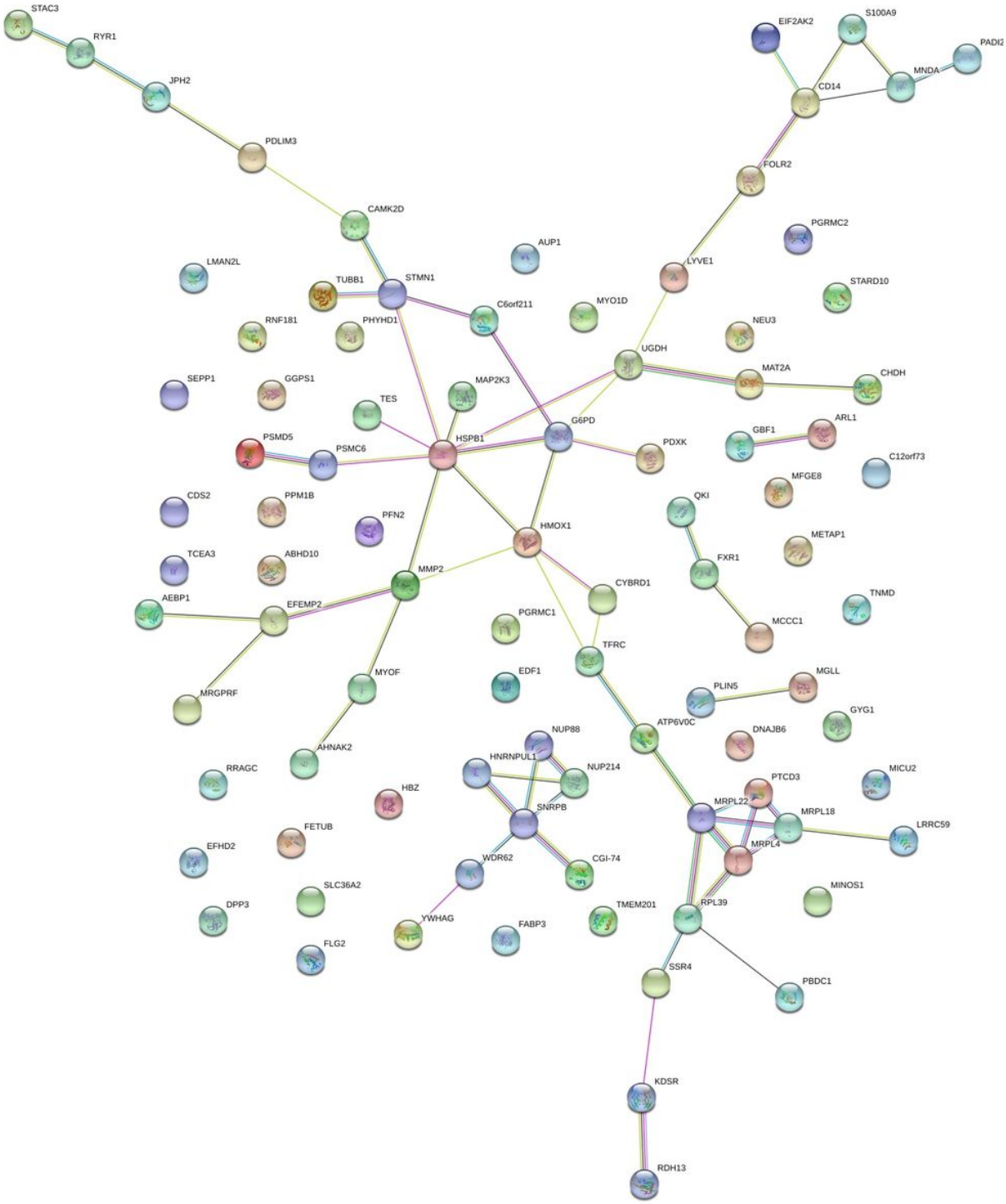

Figure 8

PPI network of common differential proteins The balls represent the proteins nodes. Circle represents gene; line represents PPI between genes, and results inside the circle represent protein structure. Line colors stand for the evidence of PPI.

Supplementary Files

This is a list of supplementary files associated with this preprint. Click to download.

- supplementary1.doc